

## **A Consideration of High-Frequency Effects on Power Harnesses for Hybrid Electric Vehicles**

Yoshio Mizutani<sup>1</sup>, Tomohiro Keishi<sup>2</sup>

<sup>1</sup>*Hybrid Vehicle R&D Div., AutoNetworks Technologies, Ltd. (Sumitomo Electric Group),  
1-14 Nishisuehiro-cho, Yokkaichi, Mie 510-8503 Japan, yoshio-mizutani@gate.sws.co.jp*

<sup>2</sup>*Analysis Technology Research Center, Sumitomo Electric Industries, Ltd.,  
1-1-3 Shimaya, Konohana-ku, Osaka 554-0024 Japan, keishi-tomohiro@sei.co.jp*

---

### **Abstract**

In HEVs (Hybrid Electric Vehicles) and EVs (Electric Vehicles), rather high voltage and current are used for the power train. Specifically, the frequency of inverter output current is in the kHz-range, and high-frequency effects (Skin effect & Proximity effect) appear in conductors (harnesses or bus-bars). These effects are phenomena particular to alternating current. The skin effect is a phenomenon in which flowing current concentrates near the surface of the conductor, while the proximity effect occurs in a way that the current paths are attracted or repelled mutually by the interaction between currents flowing in the individual conductors. Both effects appear noticeably at high-frequencies, increasing the impedance of the conductors. Harness design that takes into account these high-frequency effects is more important than ever. The distributions of current density and magnetic flux density of conductors were computed using the numerical analysis of magnetic fields and eddy-currents based on the finite element method (FEM) in frequency domain. The impedance of conductors with circular and rectangular cross-section, such as resistance  $R$  and self-inductance  $L$ , was calculated using applied voltage and resultant current based on the distribution of current density. And accuracy of the FEM was verified by comparing with theoretical or experimental results. Calculated results of the impedance for different cross-sections and various layouts of conductors applicable to actual EV are compared. And then, the impedance of conductors hooked up a load (motor) was calculated and the difference between with load and without load was discussed.

---

*Keywords:* simulation, finite element calculation, current density

---

### **1 Introduction**

In HEVs and EVs, the frequency of inverter output current is in the kHz-range, and high-frequency effects (Skin effect and Proximity effect) appear in conductor (harnesses or bus-bars). When we consider the future trend of high voltage system such as HEVs, PHEVs (Plug-in

HEVs) and EVs, this current will be increasing. Additionally the possible space of harness will be narrow. In this case, the high-frequency effects may be not significantly disregarded, because of these effects increase the impedance of conductor. Therefore harness design in consideration of these high-frequency effects may become very important. In order to solve this concern, we computed the high-frequency impedance of

single-phase conductor and 3-phase conductors based on the numerical analysis of magnetic fields and eddy-currents.

## 2 Impedance of basic conductors

### 2.1 Impedance of circular cross-section conductor

#### 2.1.1 Skin effect and theoretical value

In a straight wire of a circular cross-section as shown in Fig.1, the voltage is applied to longitudinal both end faces of this conductor. In this case, the theoretical value of the current density is given by eq.(1) as a function of radius  $r$  [1][2],

$$i(r) = i_z(r) = \frac{kI}{2\pi a} \frac{J_0(kr)}{J_1(ka)} \quad (1)$$

where  $I$  is the total current,  $a$  is the radius of conductor,  $J_0$  and  $J_1$  represent the Bessel functions of first kind of each order 0 and 1.  $k$  is the complex number as given by eq.(2).

$$k = \sqrt{-j\sigma\mu\omega} \quad (2)$$

where  $j = \sqrt{-1}$ ,  $\sigma$  is the conductivity of the conductor,  $\mu$  is the magnetic permeability of the conductor, and  $\omega (=2\pi f)$  is the angular frequency of the applied voltage.

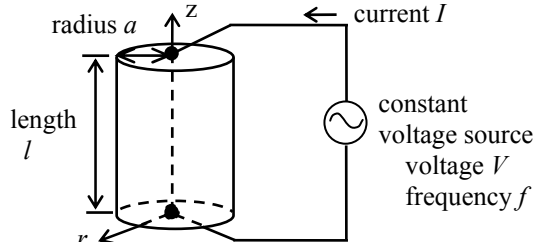


Figure 1: A straight wire of a circular cross-section

The theoretical values of the resistance  $R[\Omega]$  and self-inductance  $L[H]$  in Fig.1 are given by eqs.(3)~(7) [3][4].

$$R + j\omega L_i = \frac{jR_s}{\sqrt{2\pi a}} \left[ \frac{\text{Ber } q + j \text{Bei } q}{\text{Ber}' q + j \text{Bei}' q} \right] l \quad (3)$$

where Ber and Bei represent the Kelvin functions of first kind of order 0, Ber' and Bei' represent the derivatives of the Kelvin functions of first kind of order 0.

$$L_e = \frac{\mu_0}{2\pi} \left[ l \ln \frac{l + \sqrt{a^2 + l^2}}{a} - \sqrt{a^2 + l^2} + a \right] \quad (4)$$

$$L = L_i + L_e \quad (5)$$

where  $L$ ,  $L_i$ , and  $L_e$  are the self-inductance, the internal-inductance, and the external-inductance [H] each,  $a$  is the radius of conductor [m],  $l$  is the length of conductor [m],  $\omega=2\pi f$  is the angular frequency [rad/s], and  $\mu_0=4\pi\times10^{-7}$  is the magnetic permeability of vacuum [H/m].

$$R_s = \frac{1}{\sigma\delta} = \sqrt{\frac{\pi f \mu}{\sigma}} \quad (6)$$

where  $R_s$  is the surface resistance [ $\Omega$ ],  $\sigma$  is the conductivity [S/m],  $\mu$  is the permeability [H/m],  $f$  is the frequency [Hz], and  $\delta$  is the skin depth [m].  $\delta$  and  $q$  are shown by eq.(7).

$$\delta = \sqrt{\frac{1}{\pi f \mu \sigma}}, \quad q = \frac{\sqrt{2}a}{\delta} \quad (7)$$

#### 2.1.2 Results of FEM analysis

In the straight wire of a circular cross-section which is shown by Fig.1, the current density distribution were computed using the numerical analysis of magnetic fields and eddy-currents based on the finite element method (FEM analysis) in frequency domain for case of the aluminium conductor (conductivity  $\sigma=3.31\times10^7$  [S/m],  $a=5[\text{mm}]$ ,  $l=1[\text{m}]$ ,  $V=1[\text{V}]$ ,  $f=1$  and  $10[\text{kHz}]$ ). The radius direction distributions of normalized current density  $i(r)/i(a)$  by current density  $i(a)$  of the conductor surface ( $r=a$ ) are shown by dots in Fig.2. And the theoretical values calculated using eq.(1) are shown by lines in Fig.2. And then the theoretical values of impedance calculated using eqs.(3)~(7) are shown in Table 1.

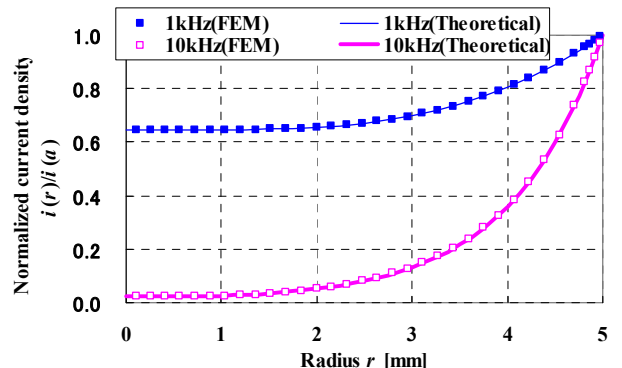


Figure 2: The current density distribution of a straight wire of a circular cross-section

As shown Fig.2, the current density of conductor surface is increased by the skin effect, and this phenomenon is remarkable at high frequency. From Fig.2 and Table 1, the FEM analyses are in good agreement with the theoretical values. Therefore we can consider computing with good accuracy by FEM analysis.

Table 1: The impedance of a straight wire of a circular cross-section

	Resistance [mΩ]		Self-inductance [μH]	
$f$ [kHz]	1	10	1	10
Theory	0.464	1.203	1.049	1.049
FEM	0.458	1.205	1.119	1.091

DC resistance : 0.385[mΩ],  $f$ : Frequency

## 2.2 Impedance of two parallel straight wires of a circular cross-section

### 2.2.1 Theoretical value of self-inductance

As shown Fig.3, two straight wires of a circular cross-section are arranged in parallel. For this case, theoretical value of self-inductance is given by eq.(8) [4].

$$L = \frac{l\mu_0}{\pi} \left( \ln \frac{d}{a} + \frac{1}{4} \right) \quad (8)$$

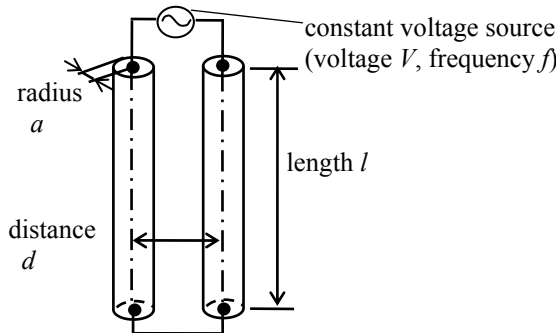


Figure 3: Two parallel straight wires of a circular cross-section

### 2.2.2 Measurement result of self-inductance

In the two parallel straight wires of a circular cross-section which is shown by Fig.3, the frequency property of self-inductance that is measured by LCR meter at the constant voltage source is shown in Fig.4 for case of copper conductor (conductivity  $\sigma=5.80 \times 10^7$  [S/m],  $a=5$  [mm],  $d=20, 40, 60, 80$  and  $100$  [mm],  $l=1$  [m]),  $V=1$  [V],  $f=1, 10, 100$  and  $200$  [kHz].

Table 2: The impedance of two parallel straight wires of a circular cross-section

	Resistance [mΩ]	Self-inductance [μH]
Theory	—	1.30
Measure	—	1.35
FEM	0.642	1.26

DC resistance : 0.440[mΩ],  $f=1$  [kHz]

### 2.2.3 Results of FEM analysis

Table 2 shows computed impedance by FEM analysis for case of copper conductor ( $a=5$  [mm],  $d=100$  [mm],  $l=1$  [m]),  $V=1$  [V],  $f=1$  [kHz] in Fig.3.

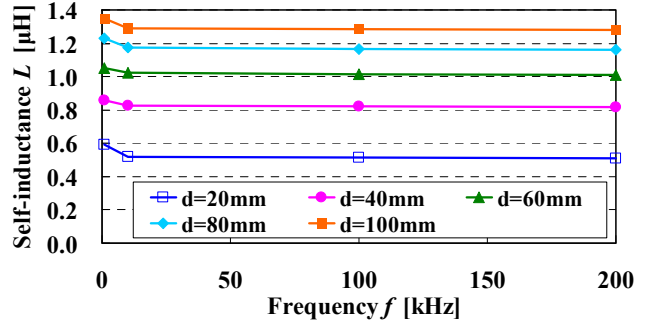


Figure 4: Measured self-inductance of two parallel straight wires of a circular cross-section ( $a=5$  [mm],  $l=1$  [m])

## 2.3 Impedance of two parallel conductors with a rectangular cross-section

### 2.3.1 Results of FEM analysis

In the two parallel conductors with a rectangular cross-section which is shown Fig.5, the current density distribution and the impedance were computed by FEM analysis for case of the aluminium conductor (conductivity  $\sigma=3.31 \times 10^7$  [S/m],  $a=10$  [mm],  $b=2$  [mm],  $d=1$  [mm],  $l=1$  [m]),  $V=1$  [V],  $f=1$  and  $10$  [kHz].

The current density distributions on cross-section of conductor for the series connection and the parallel connection are shown in Fig.6 and Fig.7, respectively. The current density for series connection is increased at the both edges of opposed surface of conductors by the skin effect and the proximity effect. And the current density for parallel connection is increased at the both edges of outer periphery of conductors. This trend is remarkably appeared at higher frequency.

Fig.8 shows the result of impedance analysis of conductor for gap  $d=1, 5, 9$  [mm] on the series connection. For the same gap, the resistance is increase, the self-inductance is decrease, and the impedance is increase with increasing frequency. For the gap is increasing, the resistance is increase at  $1$  [kHz] and is decrease at  $10$  [kHz], the self-inductance and the impedance are increase.

Table 3 shows the result of impedance analysis of conductor for gap  $d=1$  [mm] on the parallel connection.

It was possible to compute the impedance of conductor with a rectangular cross-section by

FEM analysis.

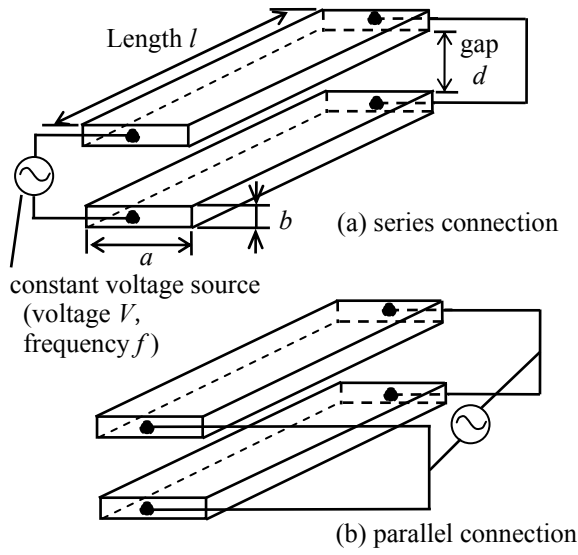


Figure 5: Two parallel conductors with a rectangular cross-section (a) series connection (b) parallel connection

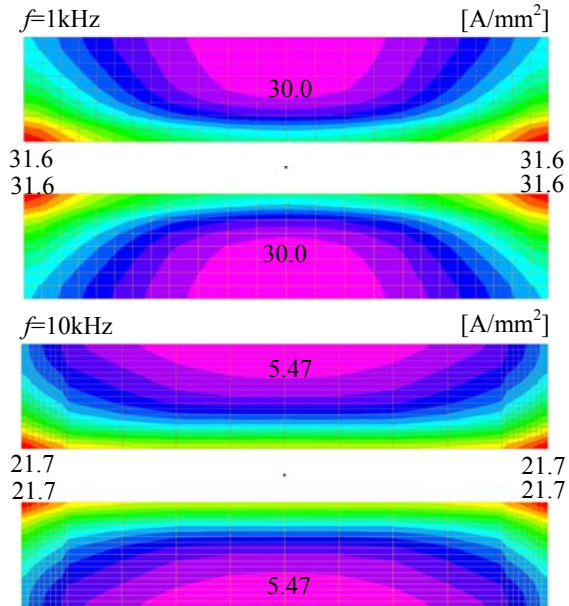


Figure 6: Current density distribution of two parallel conductors with a rectangular cross-section (series connection)

Table 3: Calculated impedances of two parallel conductors with a rectangular cross-section (parallel connection)

$f$ [kHz]	Resistance [mΩ]	Inductance [μH]	Impedance [mΩ]
1	0.800	1.10	6.98
10	1.64	1.08	67.9

DC resistance : 0.756[mΩ],  $f$ : Frequency

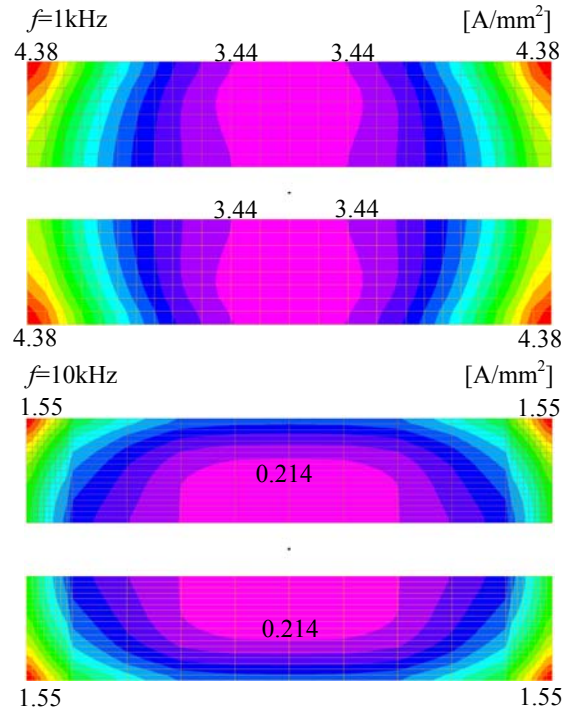


Figure 7: Current density distribution of two parallel conductors with a rectangular cross-section (parallel connection)

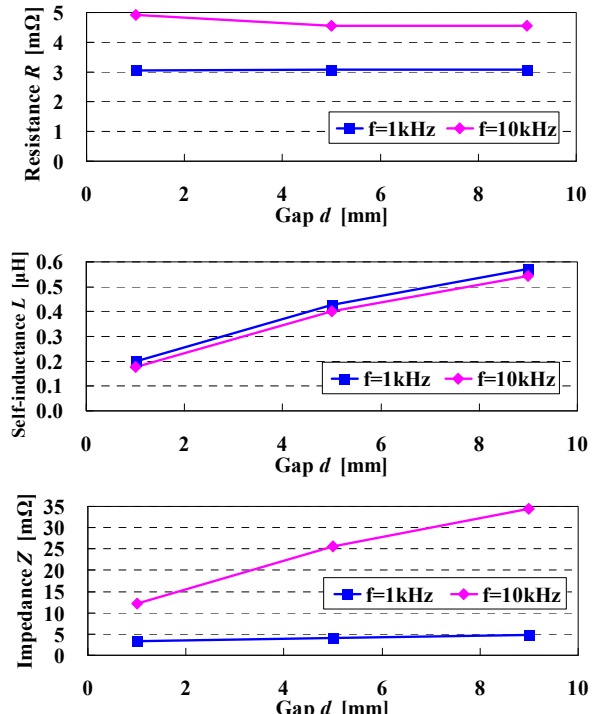


Figure 8: Calculated impedances of two parallel conductors with a rectangular cross-section (series connection) : DC resistance 3.02[mΩ]

## 2.4 Impedance of 3-phase circuit

### 2.4.1 Equilateral triangle layout of three straight wires of a circular cross-section

The FEM analysis was performed on the equilateral triangle layout of three straight wires of a circular cross-section as shown Fig.9 for applied 3-phase voltage. The current density distribution and the impedance were computed by FEM analysis for case of the aluminium conductor ( $a=5[\text{mm}]$ ,  $d=20[\text{mm}]$ ,  $l=1[\text{m}]$ ,  $V=1[\text{V}]$ ,  $f=1$  and  $10[\text{kHz}]$ ).

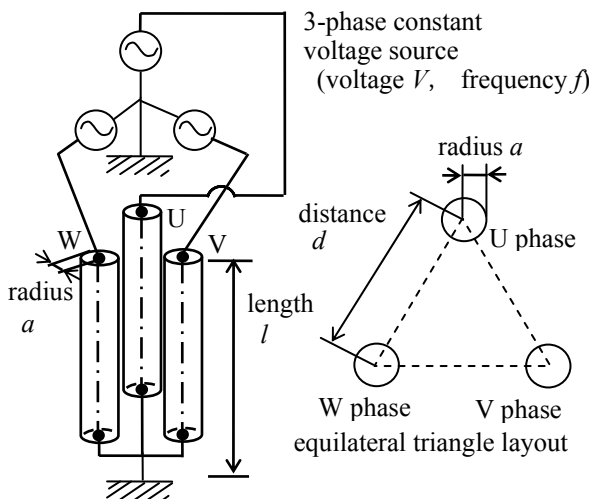


Figure 9: The equilateral triangle layout of three straight wires of a circular cross-section (3-phase)

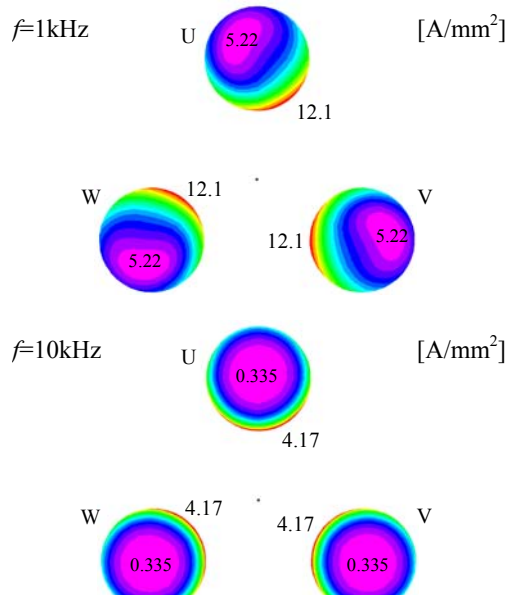


Figure 10: Current density distribution of the equilateral triangle layout of three straight wires of a circular cross-section (3-phase)

The current density distributions on cross-section of conductors are shown in Fig.10. The current density is increased at the part of opposed surface of conductors by the skin effect and the proximity effect. The patterns of current density distribution for each phases are same, these are corresponding each other with rotate 120-degrees. Table 4 shows the result of impedance analysis of conductors, these are values of each phases. The values of each phases are same each other, namely it is balanced impedance.

Table 4: Calculated impedance of the equilateral triangle layout of three straight wires of a circular cross-section (3-phase)

$f$ [kHz]	Resistance [mΩ]	Inductance [μH]	Impedance [mΩ]
1	0.503	0.314	2.03
10	1.40	0.278	17.6

DC resistance :  $0.385[\text{mΩ}]$ ,  $f$ : Frequency

### 2.4.2 Vertical layout conductors with a rectangular cross-section

The FEM analysis was performed on the three vertical layout conductors with a rectangular cross-section as shown Fig.11 for applied 3-phase voltage. The current density distribution and the impedance were computed by FEM analysis for case of the aluminium conductor ( $a=10[\text{mm}]$ ,  $b=2[\text{mm}]$ ,  $d=1, 5$  and  $9[\text{mm}]$ ,  $l=1[\text{m}]$ ,  $V=1[\text{V}]$ ,  $f=1$  and  $10[\text{kHz}]$ ).

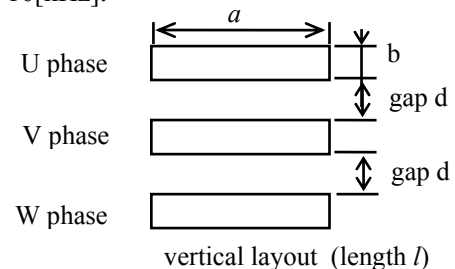


Figure 11: Three vertical layout conductors with a rectangular cross-section (3-phase)

The current density distributions on cross-section of conductors are shown in Fig.12. The current density is increased at the part of opposed surface of conductors by the skin effect and the proximity effect. The patterns of current density distribution are not symmetry between the U phase and the W phase. And the pattern of the V phase is not vertical symmetry. The impedance is evaluated by the positive-phase impedance (positive-phase resistance and positive-phase inductance) using the method of symmetrical coordinates[5] based on the results of FEM analysis due to asymmetric layout. Fig.13 shows the calculation result of the

positive-phase impedance.

We consider that calculation of the impedance is possible using FEM analysis for 3-phase circuit.

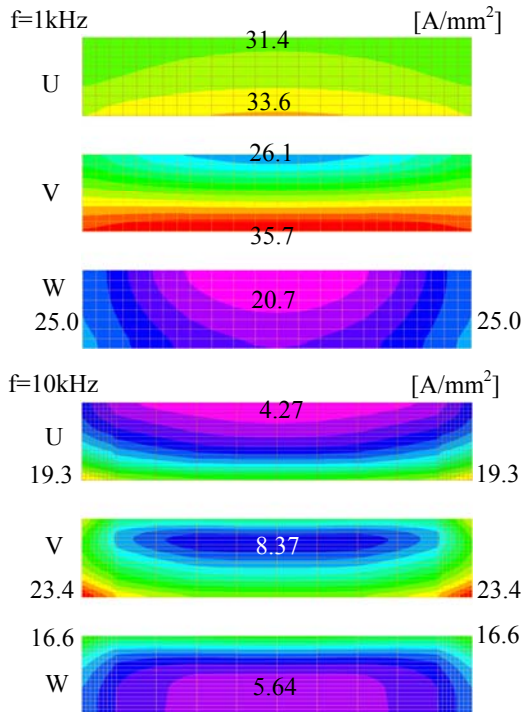


Figure 12: Current density distribution of three vertical layout conductors with a rectangular cross-section (3-phase)

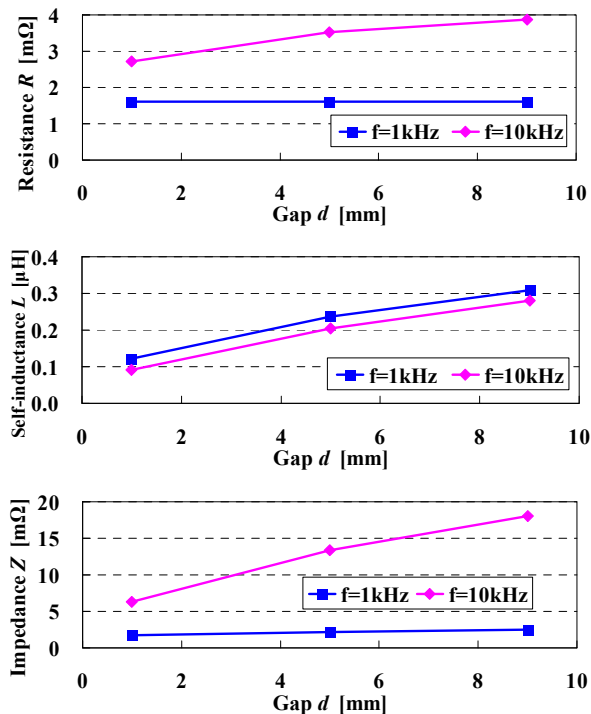


Figure 13: Calculated positive-phase impedances of three vertical layout conductors with a rectangular cross-section (3-phase) : DC resistance 1.51[mΩ]

### 3 Relations between cross-sectional shape, layout, gap of conductor and impedance

#### 3.1 Cross-sectional shape of straight conductor and impedance

The impedances of straight conductors are analyzed for same cross-sectional area and some cross-sectional shapes that are circular, square and rectangular as shown in Fig.14. The cross-sectional shape of the aluminium conductor with length  $l=1[\text{m}]$  and cross-sectional area  $20[\text{mm}^2]$  are circular ( $5.05\text{mm}\Phi$ ), square ( $4.47\text{mm}^2$ ), rectangular (width $\times$ thickness:  $6.67\text{mm}\times3\text{mm}$ ,  $10\text{mm}\times2\text{mm}$ ,  $20\text{mm}\times1\text{mm}$  and  $40\text{mm}\times0.5\text{mm}$ ). The current are computed by FEM analysis for condition of applied voltage ( $V=1[\text{V}]$ ,  $f=1$  and  $10[\text{kHz}]$ ) to the both end of conductor. And then the impedance is calculated by dividing the applied voltage by the computed current. The results of impedance analysis are shown in Fig.15 and Table 5.

FastHenry[6][7] and SIMIAN[8] are developed as software for impedance calculation of conductor. Table 6 and Table 7 show the results of impedance calculation for the straight conductors using these software. The results of FEM analysis for resistance and self-inductance are good according to the results of FastHenry and SIMIAN. Therefore we consider that the impedance can be analyzed with good accuracy by FEM analysis.

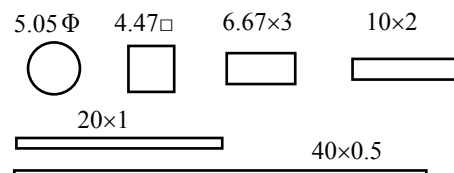


Figure 14: Different shapes of same cross-sectional area ( $20\text{mm}^2$ ) [mm]

For same cross-sectional shape, the resistance and the impedance are increased, and the self-inductance is decreased with the higher of frequency. For the frequency  $f=10[\text{kHz}]$ , the resistance, the inductance and the impedance are decreased with the thinner of thickness of rectangular cross-section. By contrast, the impedance is nearly-unchanged with change of the aspect-ratio of rectangular at frequency  $f=1[\text{kHz}]$ .

Also frequency independent self-inductance can be calculated from the rectangular cross-sectional shape using Ruehli's formula[9][10], Grover's

formula[9]. This calculation result is shown in Table 8. The self-inductance  $L$  is decreased with the thinner thickness of rectangular cross-section. This tendency is according to the result of FEM analysis.

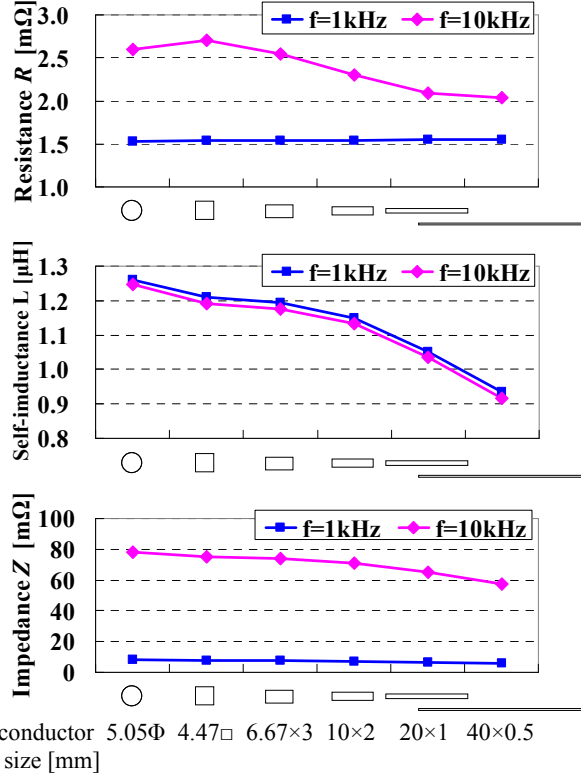


Figure 15: The impedance of straight conductors with a different shape of same cross-sectional area (FEM results)

Table 5: The impedance of straight conductors with a different shape of same cross-sectional area (FEM results)

Cross-section size[mm]	$f$ [kHz]	Resistance $R$ [mΩ]	Self-inductance $L$ [μH]
circle 5.05Φ	1	1.533	1.259
	10	2.599	1.247
square 4.47×4.47	1	1.539	1.209
	10	2.706	1.191
rectangle 6.67×3	1	1.539	1.194
	10	2.546	1.176
rectangle 10×2	1	1.544	1.150
	10	2.296	1.133
rectangle 20×1	1	1.547	1.052
	10	2.090	1.035
rectangle 40×0.5	1	1.547	0.9337
	10	2.040	0.9168

DC resistance : 1.51[mΩ]  $f$ : Frequency

Table 6: The impedance of straight conductors with a different shape of same cross-sectional area (FastHenry results)

Cross-section size[mm]	$f$ [kHz]	Resistance $R$ [mΩ]	Self-inductance $L$ [μH]
square 4.47×4.47	1	1.537	1.181
	10	2.719	1.164
rectangle 6.67×3	1	1.537	1.165
	10	2.539	1.148
rectangle 10×2	1	1.541	1.122
	10	2.281	1.105
rectangle 20×1	1	1.543	1.010
	10	2.064	0.9948
rectangle 40×0.5	1	1.543	0.8804
	10	1.988	0.8656

$f$ : Frequency

Table 7: The impedance of straight conductors with a different shape of same cross-sectional area (SIMIAN results)

Cross-section size[mm]	$f$ [kHz]	Resistance $R$ [mΩ]	Self-inductance $L$ [μH]
circle 5.05Φ	1	1.533	1.246
	10	2.628	1.230
square 4.47×4.47	1	1.548	1.253
	10	2.880	1.228
rectangle 6.67×3	1	1.553	1.230
	10	2.512	1.211
rectangle 10×2	1	1.548	1.184
	10	2.230	1.166
rectangle 20×1	1	1.545	1.071
	10	2.072	1.055
rectangle 40×0.5	1	1.536	0.9384
	10	1.964	0.9232

$f$ : Frequency

Table 8: Ruehli's formula and Grover's formula results

Cross-section size $w\times t$ [mm]	Self-inductance $L$ [μH]	
	Ruehli's formula	Grover's formula
square 4.47×4.47	1.182	1.083
rectangle 6.67×3	1.166	1.067
rectangle 10×2	1.123	1.024
rectangle 20×1	1.012	0.9123
rectangle 40×0.5	0.8825	0.7820

Here, we note to AC (alternate current) resistance of straight conductors with a rectangular cross-section. The AC resistance is affected by skin depth. The skin depth  $\delta$ [m] is calculated by eq.(7). The skin depth of the aluminium conductor is shown in Table 9.

Table 9: Skin depth of the aluminium conductor

Frequency $f$ [kHz]	Skin depth $\delta$ [mm]
1	2.77
10	0.875

The graph for 10[kHz] of Fig.15 shows that the resistance is decreased with the thinner of thickness of rectangular cross-section. For the same cross-sectional area, Fig.16 shows that the resistance drop is nearly saturated at thickness less than or equal to the skin depth. This phenomenon is caused by the skin effect that effective cross-sectional area for current flow is decreased with the higher of frequency. Thereby AC resistance for high frequency is larger than DC resistance on large cross-sectional area conductor, and the temperature rise for Joule-heat is large, too. Therefore this phenomenon should be considered on design of conductor size.

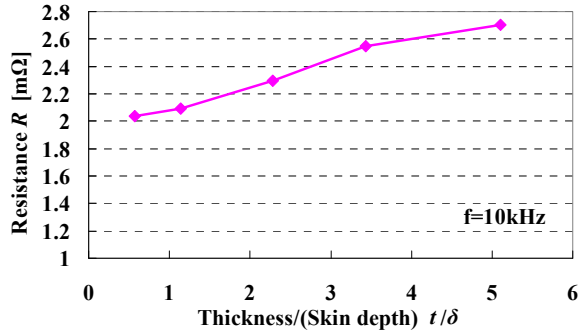


Figure 16: The relationship between the resistance and the thickness of a conductor with a rectangular cross-section.

### 3.2 Layout of conductors and impedance

Here, we discuss the 3D layout of conductors with 2 right-angled bends. Their impedances are computed for some different cross-sectional layouts by FEM analysis.

#### 3.2.1 Case of 3-phase circuit

The impedances of 3-phase circuit are computed for some different cross-sectional layouts as shown in Fig.17. For all layouts, the average length of conductors of each phase is 200[mm], conductor gap  $d=1$ [mm], the conductor material is aluminium and the cross-sectional shape is a rectangular. As shown in Fig.18, the one end of conductor is shorted and grounded, the 3-phase voltage source ( $V=1$ [V],  $f=1$ , 10[kHz]) is connected to other end of conductor. FEM analysis is carried out on this condition, and the impedance is calculated by dividing the applied

voltage by the computed current.

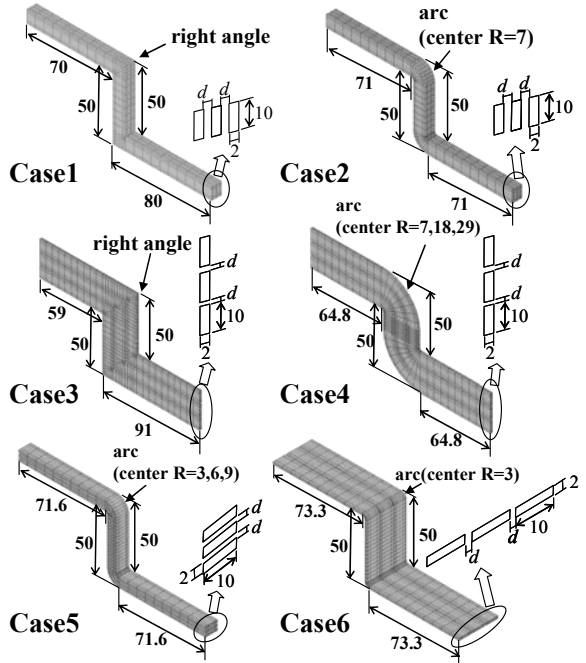


Figure 17: 3D conductor layout with different cross-sectional layouts. [mm]

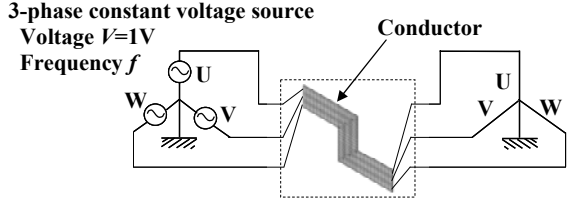


Figure 18: The electric circuit of 3-phase conductor

Fig.19 shows the positive-phase impedance obtained by result of FEM analysis. The resistance and the impedance are increased, and the inductance is decreased with the higher of frequency. Also the resistance, the inductance and the impedance can be decreased at layout adjacent to the long sides each other (Case1, Case2 and Case5), in comparison with layout adjacent to the short sides each other (Case3, Case4 and Case6) on conductor with a rectangular cross-section. For the sensitivities of the resistance and the impedance to change in frequency, the layout adjacent to the short sides each other is more sensitive than the layout adjacent to the long side each other.

### 3.3 Gap of conductors and impedance

#### 3.3.1 Vertical layout conductors with a rectangular cross section

The FEM analysis was performed on the three

vertical layout conductors with a rectangular cross-section as shown Fig.11 for applied 3-phase voltage. The impedance was computed by FEM analysis for case of the aluminium conductor ( $a=10[\text{mm}]$ ,  $b=2[\text{mm}]$ ,  $d=1, 5$  and  $9[\text{mm}]$ ,  $l=1[\text{m}]$ ),  $V=1[\text{V}]$ ,  $f=1$  and  $10[\text{kHz}]$ , and for condition of applied voltage ( $V=1[\text{V}]$ ,  $f=1$  and  $10[\text{kHz}]$ ) as shown in Fig.18.

Fig.13 shows the calculation result of the positive-phase impedance. The resistance, the inductance and the impedance are decreased with the narrower of conductor gap.

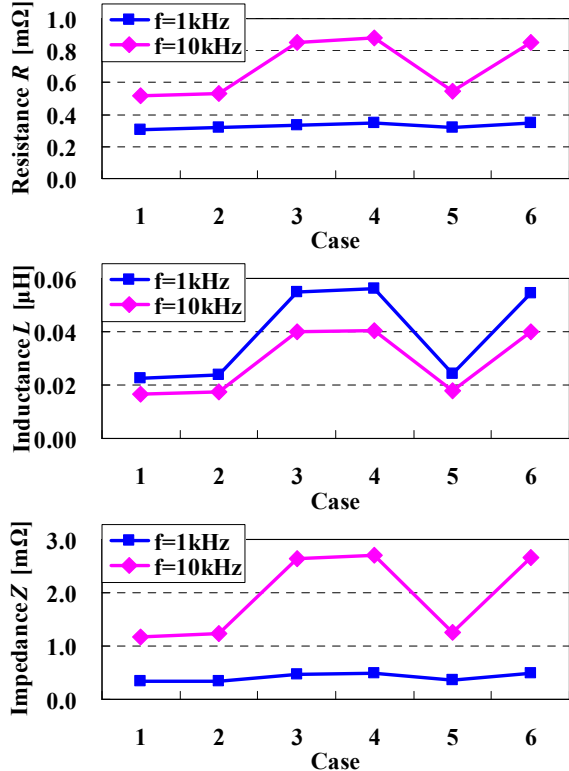


Figure 19: The positive-phase impedance of 3D conductors with different cross-sectional layouts (3-phase)

## 4 Influence of load

### 4.1 Impedance of conductor with load

In the straight wire of a circular cross-section connected to the load  $Z_L$  which is shown by Fig.20, the current density distribution were computed using FEM analysis for case of the aluminium conductor ( $a=5[\text{mm}]$ ,  $l=1[\text{m}]$ ),  $V=1[\text{V}]$ ,  $f=1$  and  $10[\text{kHz}]$ . The load  $Z_L$  used value of Table 10 which was actual measurement value of the motor. Table 11 shows the impedance obtained by result of FEM analysis. The theoretical values and results of FEM analysis for case of without the load are same to Table 1. The results of FEM

analysis for case of with the load were good according to the theoretical values and results of FEM analysis for case of without the load. This result indicates that the load  $Z_L$  does not influence to FEM analysis.

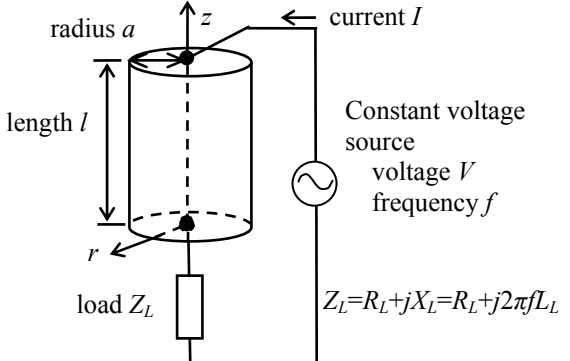


Figure 20: A straight wire of a circular cross-section

Table 10: Impedance of the load

Frequency $f$ [kHz]	Resistance $R_L$ [mΩ]	Inductance $L_L$ [μH]	Reactance $X_L$ [Ω]
1	34.3	283	1.778
10	35.0	262	16.46

$$\text{Impedance } Z_L = R_L + jX_L = R_L + j2\pi f L_L$$

Table 11: The impedance of a straight wire of a circular cross section

	Resistance [mΩ]		Self-inductance [μH]	
Frequency $f$ (kHz)	1	10	1	10
Theory	0.464	1.203	1.049	1.049
FEM	Without load	0.458	1.205	1.119
	With load	0.458	1.200	1.110

$$\text{DC resistance : } 0.385[\text{mΩ}]$$

## 4.2 Impedance of 3-phase circuit

### 4.2.1 Equilateral triangle layout of three straight wires of a circular cross-section

The FEM analysis was performed on the equilateral triangle layout of three straight wires of a circular cross-section as shown Fig.21 for applied 3-phase voltage. The current density distribution and the impedance were computed by FEM analysis for case of the aluminium conductor ( $a=5[\text{mm}]$ ,  $d=20[\text{mm}]$ ,  $l=1[\text{m}]$ ),  $V=1[\text{V}]$ ,  $f=1$  and  $10[\text{kHz}]$ , and with the loads as shown Table 10. Table 12 shows the result of the impedance analysis of conductors, these are values of each phases. The values of each phases were same each

other, namely it was balanced impedance. The results of FEM analysis for case of with the loads were good according to the results of FEM analysis for case of without the loads.

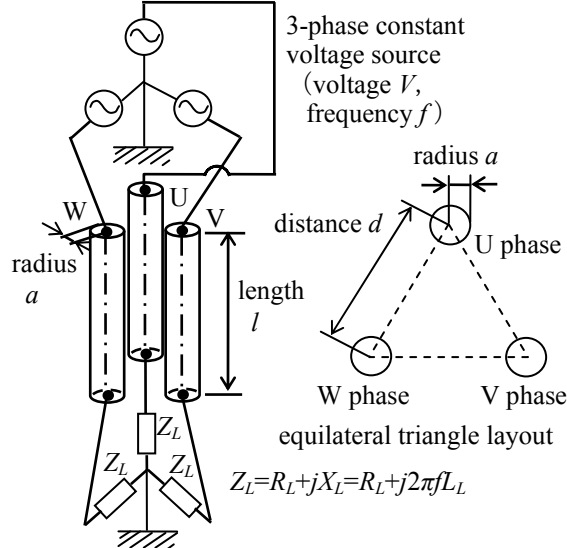


Figure 21: The equilateral triangle layout of three straight wires of a circular cross-section (3-phase)

Table 12: Calculated impedance of the equilateral triangle layout of three straight wires of a circular cross section (3-phase)

FEM	$f$ [kHz]	Resistance [mΩ]	Inductance [μH]	Impedance [mΩ]
without loads	1	0.503	0.314	2.03
	10	1.40	0.278	17.6
With loads	1	0.503	0.304	1.98
	10	1.39	0.267	16.8

DC resistance : 0.385[mΩ]

#### 4.2.2 Vertical layout conductors of a rectangular cross-section

The FEM analysis was performed on the three vertical layout conductors with a rectangular cross-section as show Fig.11 for applied 3-phase voltage. The current density distribution and the impedance were computed by FEM analysis for case of the aluminium conductor ( $a=10[\text{mm}]$ ,  $b=2[\text{mm}]$ ,  $d=1, 5$  and  $9[\text{mm}]$ ,  $l=1[\text{m}]$ ) connected to the 3-phase voltage source ( $V=1[\text{V}]$ ,  $f=1$  and  $10[\text{kHz}]$ ) and the loads as show Fig.22, the values of loads are shown in Table 10.

##### 3-phase constant voltage source

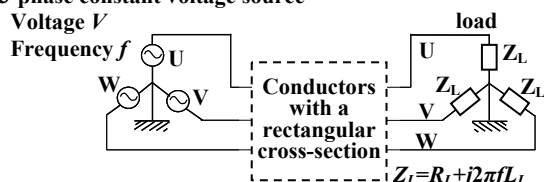


Figure 22: The electric circuit of 3-phase conductors with a rectangular cross-section

Fig.23 shows the result of the impedance analysis of conductors, these are values of each phases.

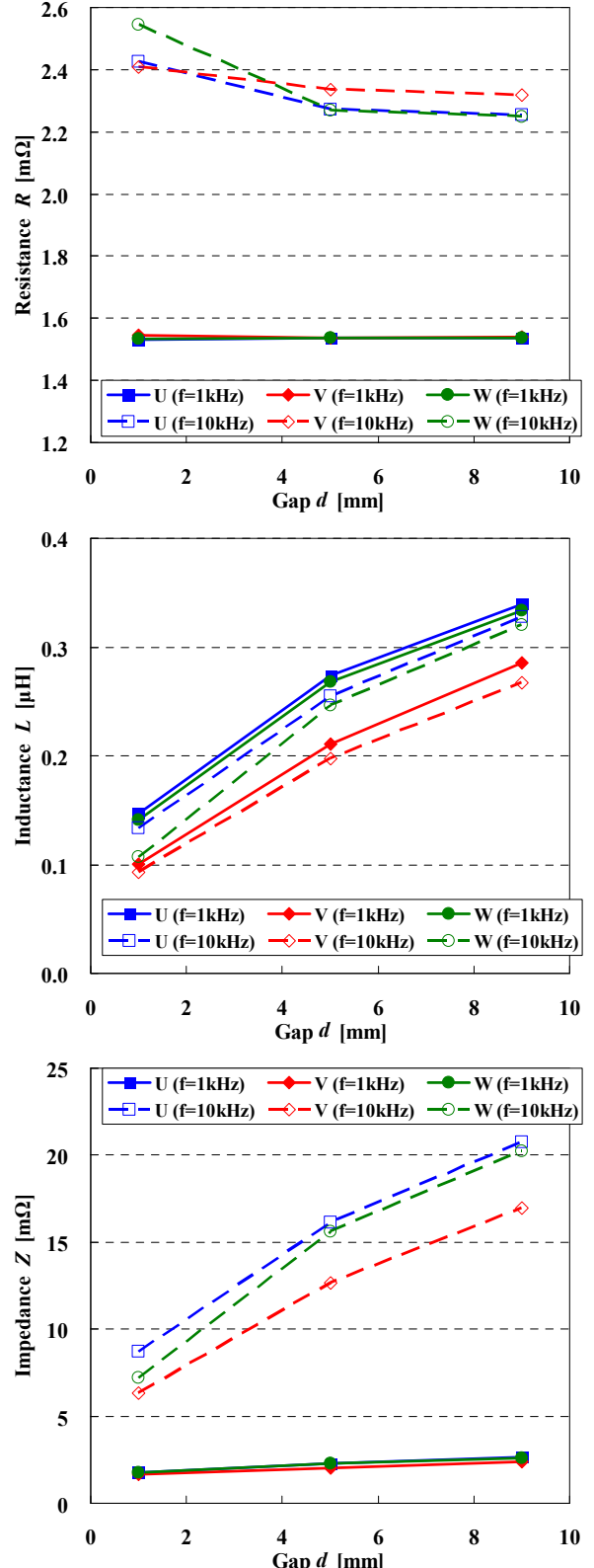


Figure 23: Calculated impedance of three vertical layout conductors of a rectangular cross-section (3-phase)

Fig.24 shows the voltage drop phasor diagrams of applied voltage, current, resistance and reactance on circuit including conductors and loads. In the circuit with the loads, the absolute values of each phase current are nearly equal to each other and the current phase delay from the voltage by 90 degrees. Therefore the absolute values of each phase impedance on circuit including conductors and loads are nearly equal to each other.

Also, Fig.25 shows the voltage drop phasor diagrams on circuit without loads. Fig.25 suggests that the each phase impedances (resistance and reactance) are different. When the load like the motor is connected to circuit, the influence of difference of impedance on each phase conductor for each circuit-current is very weak.

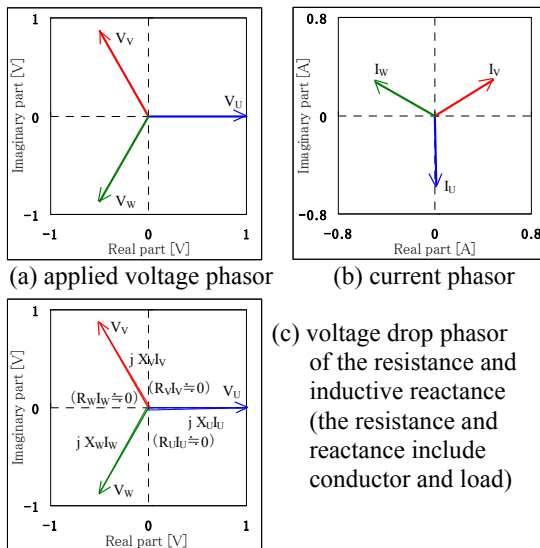


Figure 24: Voltage and current phasor of rectangular conductor circuit with loads ( $f=1\text{kHz}$ ,  $d=1\text{mm}$ )

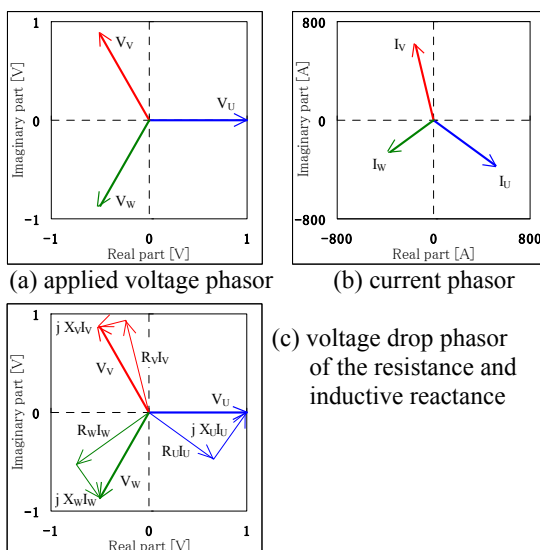


Figure 25: Voltage and current phasor of rectangular conductor circuit without loads ( $f=1\text{kHz}$ ,  $d=1\text{mm}$ )

## 5 Conclusion

We carried out computing the current density distribution and the impedance for conductor using the numerical analysis of magnetic fields and eddy-currents based on the finite element method (FEM analysis).

- Their results are in good agreement with the theoretical values and measurement values.
- We can consider computing with good accuracy by FEM analysis.
- The current density distribution is eccentrically-located by the skin effect and the proximity effect for applied single-phase and 3-phase voltage to conductor.
- The AC resistance for high frequency is larger than DC resistance on large cross-sectional area conductor due to the high frequency effect. Thereby for large current circuit, the temperature rise for Joule-heat is large, too. Therefore this phenomenon should be considered on design of conductor size.
- In the 3D layout conductors of a rectangular cross-section, the impedance can be minimized at layout adjacent to the long sides each other.

Also we carried out computing the impedance of conductor connected to the load.

- The current of conductor is determined by the impedance of load, due to the impedance of conductor is sufficiently-small compared to the impedance of load. Namely, the impedance of conductor has little influence on the impedance of circuit.

## Acknowledgments

The authors would like to thank Toshiro Shimada, who retired from Sumitomo Electric Industries in 2010, for his considerations and suggestions.

## References

- [1] Setsuzou Takeyama, *Phenomenal Theory of Electricity and Magnetism*, ISBN 3054-2049-7924, Maruzen Company, 1975, 397-404
- [2] Shigenobu Sunagawa, *Theoretical Electricity and Magnetism*, ISBN 4-314-00101-1, Kinokuniya Company, 1987, 178-181
- [3] S. Ramo, J.R. Whinnery and T. Van Duzer, *Fields and Waves in Communication Electronics*, ISBN 9-780471-585510, John Wiley & Sons, 1994, 182-186

- [4] Kenichi Goto , Syuuichiro Yamazaki, *Practice in Detail for Electricity and Magnetism*, ISBN 4-32003-022-2, Kyoritsu Shuppan Company, 1970, 275-276 & 285
- [5] Hiroshi Hirayama, *Theory of Electric Circuit*, ISBN 4-88686-103-2, Ohmsha, 1970, 241-245
- [6] M. Kamon, M. J. Tsuk and J. K. White, *FASTHENRY: A Multipole-Accelerated 3-D Inductance Extraction Program*, IEEE Trans. on Microwave Theory and Techniques, ISSN 0018-9480, 42(1994), 1750-1758
- [7] M. Kamon, C. Smithhisler and J. White, *FastHenry USER'S GUIDE Version 3.0*, Massachusetts Institute of Technology(1996)
- [8] S. Kim, E. Tuncer, B-T Lee and D. P. Neikirk, *SIMIAN USER'S GUIDE(Version 2.1)*, The University of Texas at Austin(1998)
- [9] H. Kim and C. C-P. Chen, *Be Careful of Self and Mutual Inductance Formulae*, Technical Report, University of Wisconsin-Madison(2001)
- [10] A. E. Ruehli, *Inductance Calculations in a Complex Integrated Circuit Environment*, IBM J. Res. Develop., ISSN 0018-8646, September(1972), 470-481

(Reference [1][2][4][5] are written in Japanese)

## Authors

 Yoshio Mizutani received a Master's degree in electrical engineering from Nagaoka University of Technology in 1991. He joined Sumitomo Electric Industries in 1991, where he worked at power cables and accessories division. He has been seconded to AutoNetworks Technologies in 2000, and since then he has been in charge of development of high-voltage wiring harness.

 Tomohiro Keishi received the BSET and Doctor's degrees, in electrical engineering from Okayama University in 1975 and 1994, respectively. He joined Sumitomo Electric Industries in 1975, where he worked at R & D division. He has been in charge of research for CAE(Computer Aided Engineering) from 1996. He is also a Professional Engineer Japan(Electrics & Electronics Engineering).